Supporting information

for

Scrutinizing particle size related bond strengthening in anatase TiO_2

Jinlong Yu,[a] Aref Mamahkel,[a] Frederik Søndergaard-Pedersen,[a] Marcel Ceccato,[b] Bo Brummerstedt Iversen[a,*]

[a]Center for Integrated Materials Research, Department of Chemistry and iNANO, Aarhus University, DK-8000 Aarhus, Denmark

[b]Interdisciplinary Nanoscience Center (iNANO), Aarhus University, DK-8000 Aarhus, Denmark

[*]Corresponding author: bo@chem.au.dk

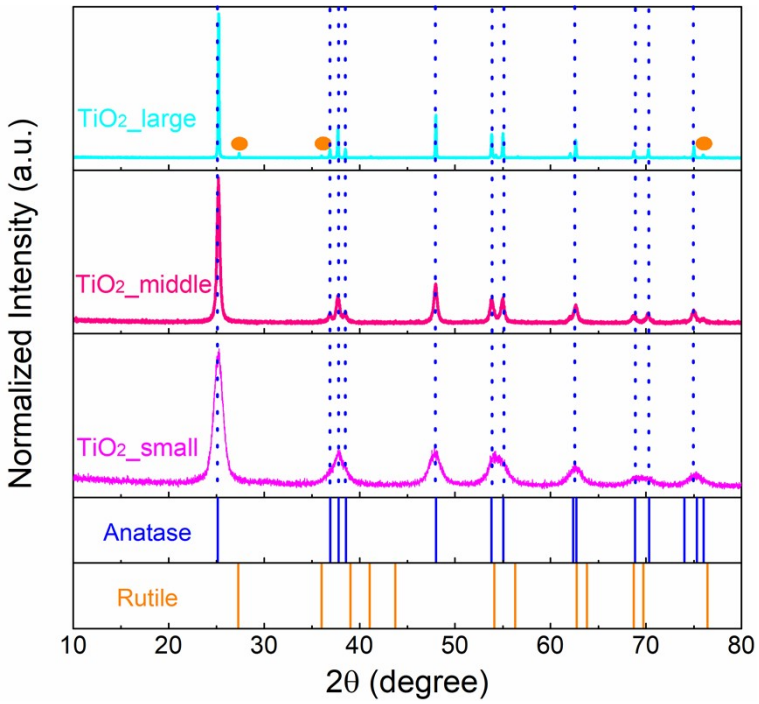

Figure S1. Room temperature laboratory PXRD patterns of synthesized anatase particles with distinct sizes (λ = 1.540590 Å). The PXRD patterns of JCPDS 00-021-1272 (anatase) and 01-078-4187 (rutile) are included for comparison.

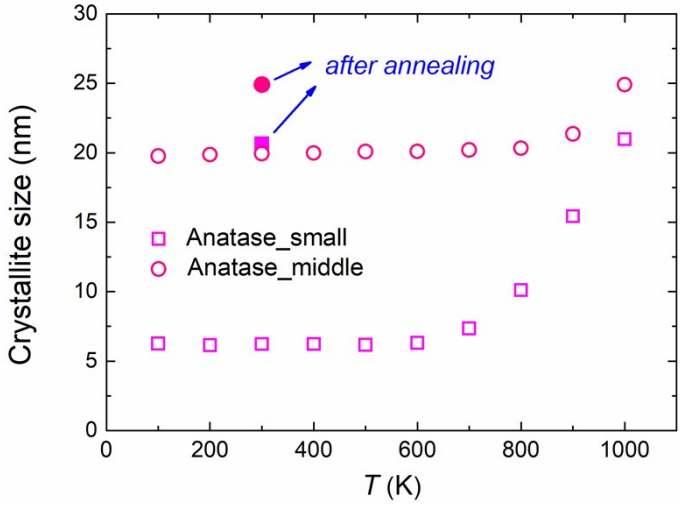

Figure S2. Variation of crystallite sizes with temperature obtained from Rietveld refinement for small and middle anatase particles.

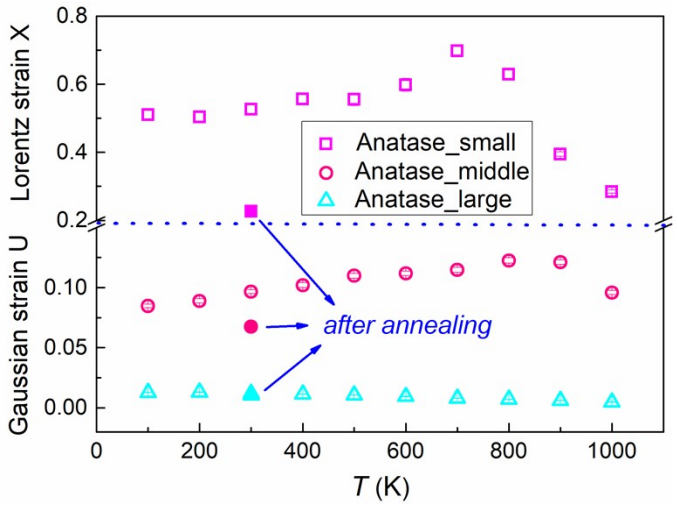

Figure S3. Variation of isotropic strains with temperature obtained from Rietveld refinement for anatase particles with distinct sizes.

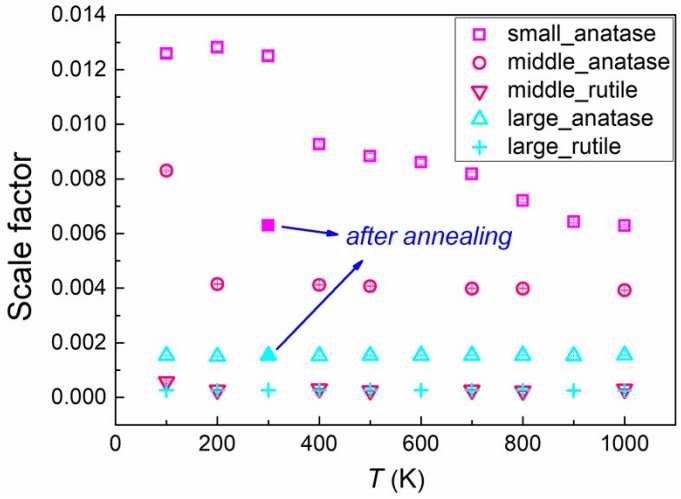

Figure S4. Variation of scale factors with temperature obtained from Rietveld refinement for TiO_2 particles with distinct sizes.

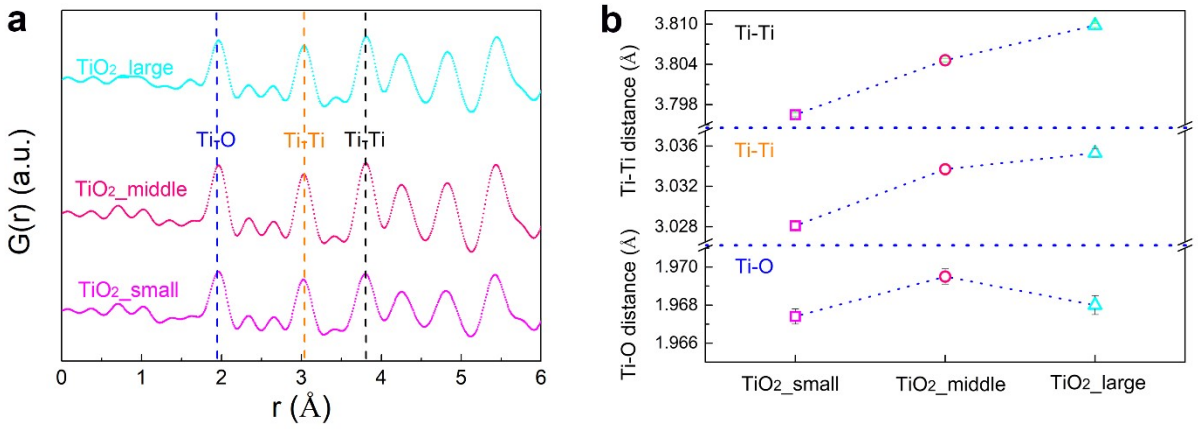

Figure S5. (a) PDFs of as-synthesized small, middle and large anatase particles calculated from total scattering data obtained at SPring8. (b) Variation of distinct interatomic distances with particle size for as-synthesized anatase particles calculated from SPring8 data.

Table S1. Unit cell parameters *a* and *c* for anatase particles with distinct sizes obtained from refinement on their PDFs calculated from SPring8 total scattering data.

	Anatase_small	Anatase_middle	Anatase_large
a/Å	3.798(2)	3.786(1)	3.7854(2)
c/Å	9.476(9)	9.507(5)	9.515(1)

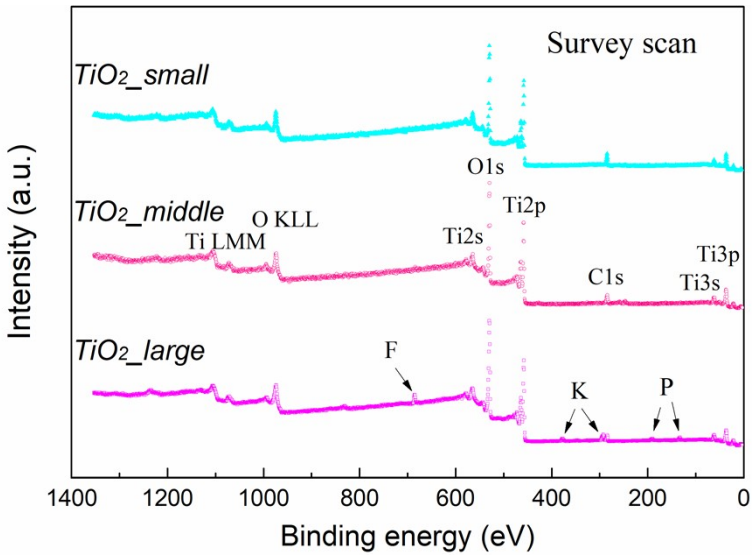

Figure S6. XPS survey scan of small, middle and large anatase particles.

Table S2. Binding energy (eV), FWHM (eV) and fitted peak area (%) for different components in high resolution O_{1s} spectra of small, middle and large anatase TiO_2 samples.

Sample	Component	Binding energy (eV)	FWHM (eV)	Fitted peak area (%)
Small TiO_2	O_{1s} (O-Ti)	530.0	1.15	82.6
	O_{1s} (-OH)	531.2	2.58	17.4
Middle TiO_2	O_{1s} (O-Ti)	529.8	1.09	83.0
	O_{1s} (-OH)	530.5	2.91	17.0
Large TiO_2	O_{1s} (O-Ti)	529.9	1.14	68.5
	O_{1s} (-OH, $(PO_4)^{3-}$)	531.4	2.75	31.5

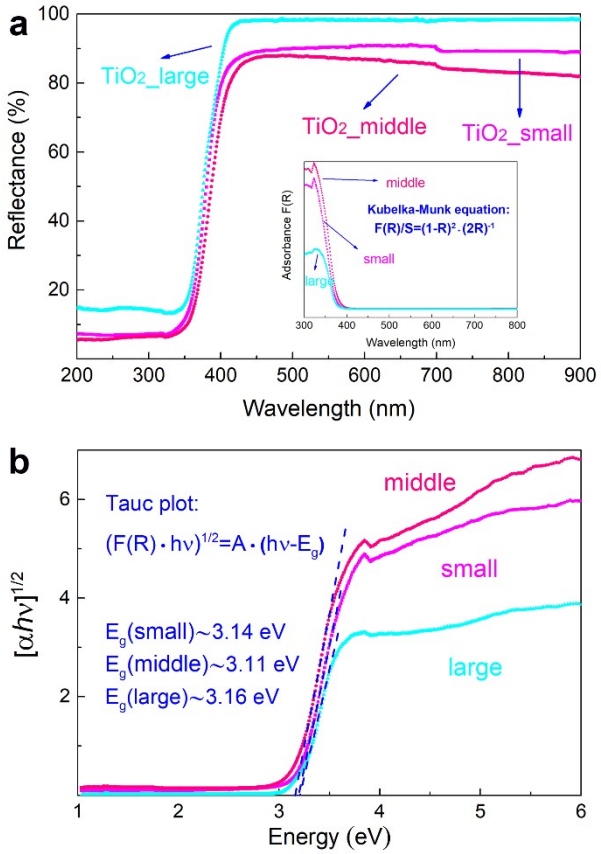

Figure S7. (a) Diffuse reflectance spectra of as-synthesized small, middle and large anatase particles. Inset is the relevant adsorption spectra converted according to Kubelka-Munk equation. (b) Tauc plot of $[F(R)\cdot h\nu]^{1/2}$ versus $h\nu$ for various anatase particles.

In order to rule out the effect of oxygen vacancies on the variation of chemical bond length and strength in as-synthesized anatase particles, optical diffuse reflectance patterns are recorded. Patterns for all three TiO_2 samples are shown in Fig. S7. The inset in Fig. S7a shows the adsorption patterns converted from relevant reflectance spectra according to Kulbelka-Munk function. The intrinsic UV-region adsorption edge, typical for TiO_2 particles, is identified for all samples. No obvious adsorption is found in the visible region for all samples. In addition, the band gap energies derived from Tauc plot (see Fig. S7b) are around

3.14 eV, 3.11 eV and 3.16 eV for the small, middle and large TiO_2 particles, respectively, all of which are much larger than that determined for black TiO_2 materials where large amount of oxygen vacancies exist.[1] Hence, the potential effect from oxygen vacancies on the chemical bond variation in as-synthesized anatase particles are ruled out.

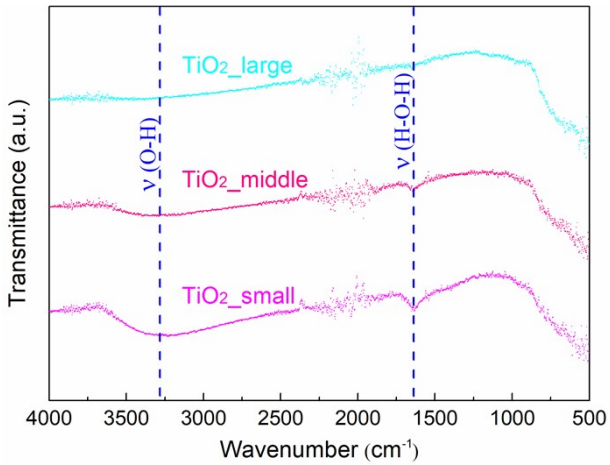

Figure S8. FT-IR spectra recorded from 500 to 4000 cm^{-1} for as-synthesized anatase particles.

FT-IR spectra of all TiO_2 particles are recorded, aiming to reveal surface functional groups. As seen in Fig. S8, two main peaks at around 3380 cm^{-1} as well as 1633 cm^{-1} assigned to typical O-H stretching mode of H_2O and H-O-H bending mode of H_2O respectively, are identified for all TiO_2 particles.[2] Due to lacking of high-resolution spectra data, detailed distinguishing of the broad band of O-H stretching mode into structural O-H and surface O-H cannot be achieved. As discussed in the main text, these –OH and hydration layers play a great role in altering the chemical bond length and strength in as-synthesized anatase particles.

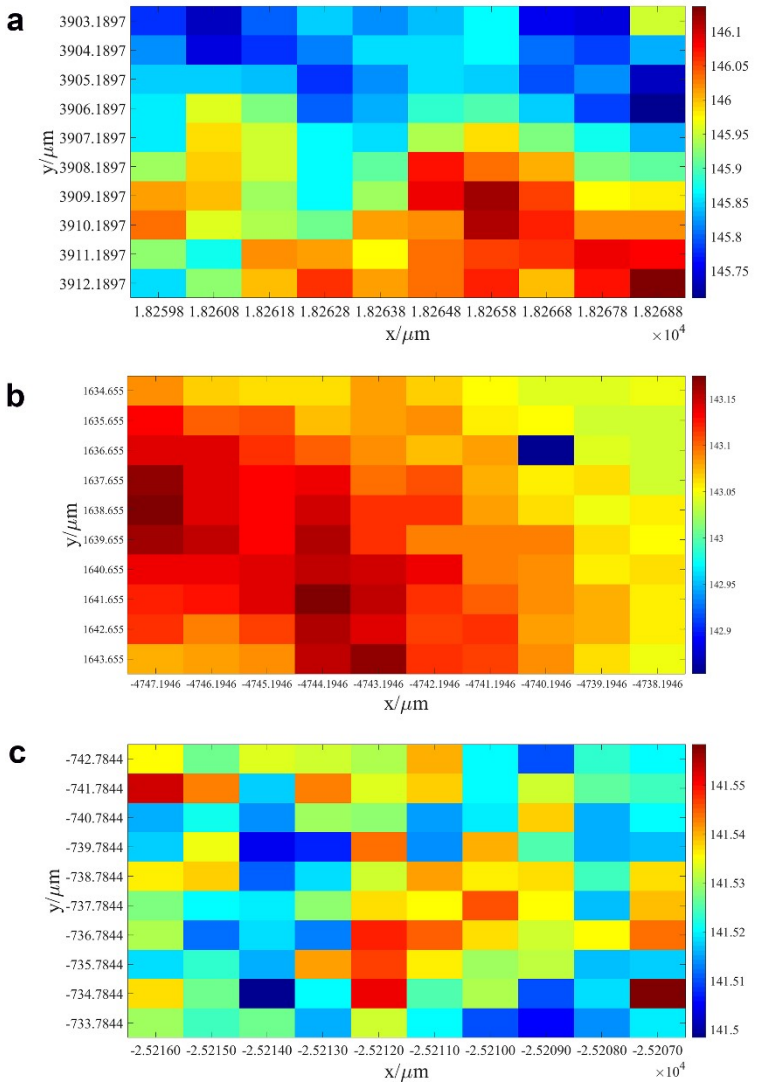

Figure S9. Mapping of Raman peak shift for E_g (~145 cm^{-1}) mode for (a) small, (b) middle and (c) large anatase particles.

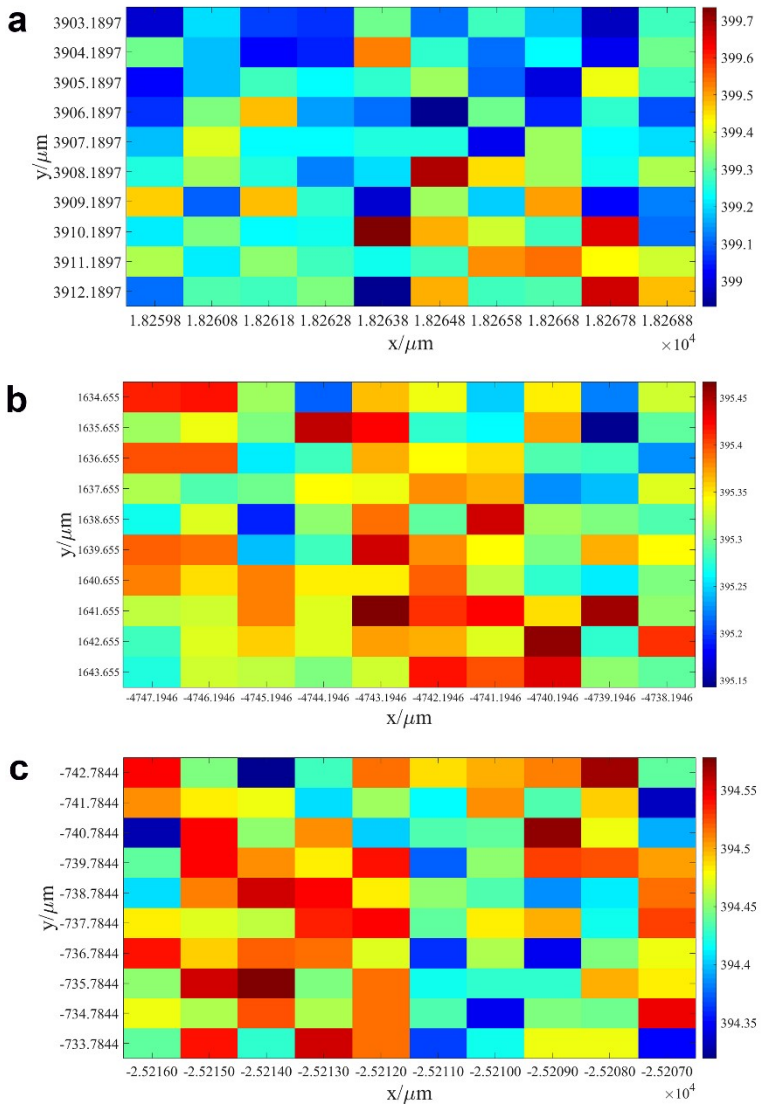

Figure S10. Mapping of Raman peak shift for B_{1g} (~397 cm^{-1}) mode for (a) small, (b) middle and (c) large anatase particles.

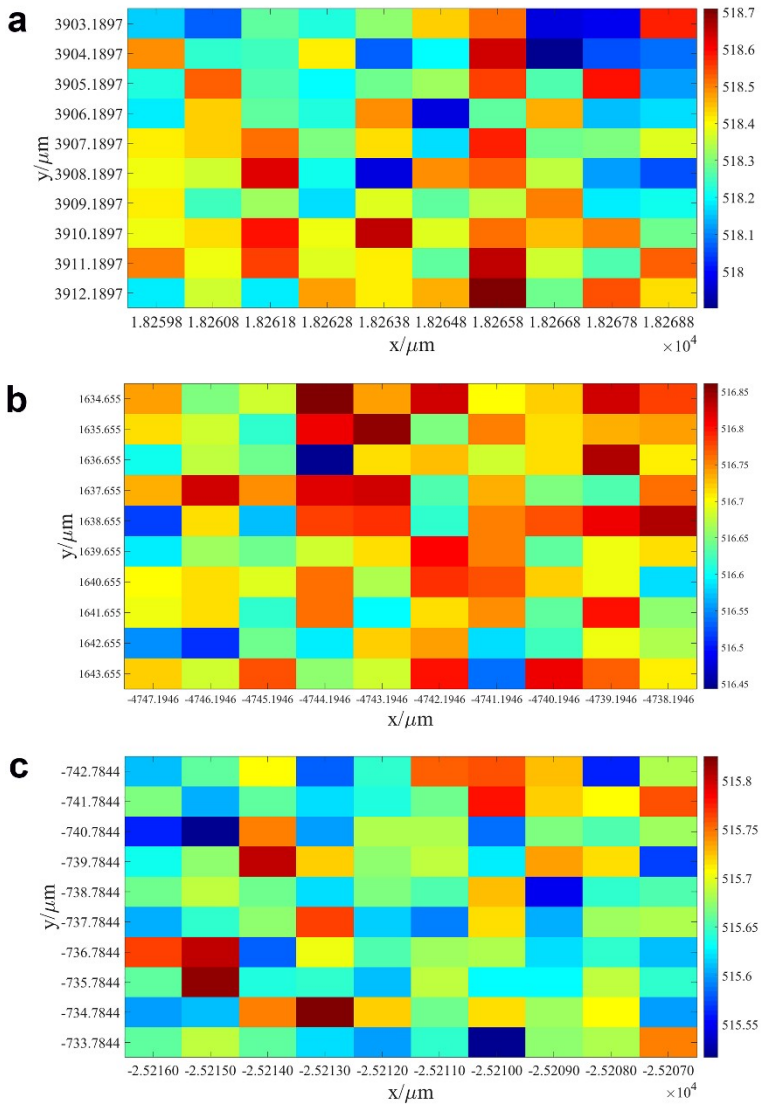

Figure S11. Mapping of Raman peak shift for A_{1g} (~513 cm^{-1}) + B_{1g} (~519 cm^{-1}) mode for (a) small, (b) middle and (c) large anatase particles.

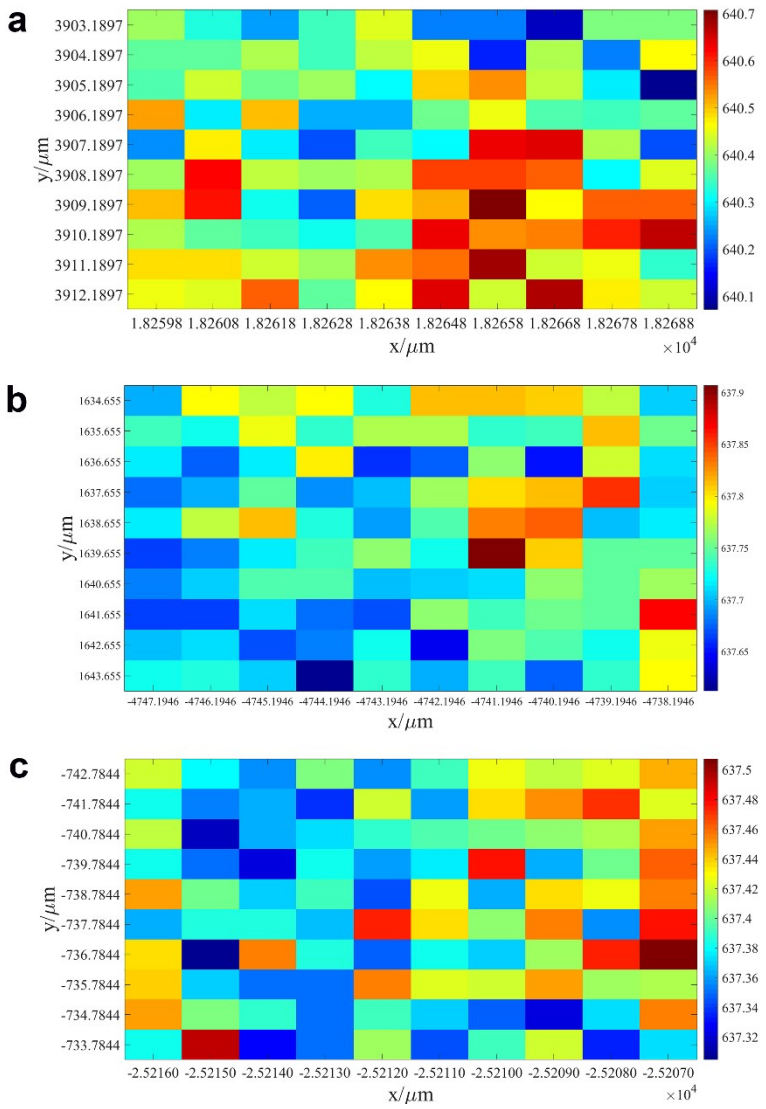

Figure S12. Mapping of Raman peak shift for E_g (~638 cm^{-1}) mode for (a) small, (b) middle and (c) large anatase particles.

References

1. X. B. Chen, L. Liu, P. Y. Yu and S. S. Mao, *Science*, 2011, **331**, 746-750.

2. Y. Ohno, K. Tomita, Y. Komatsubara, T. Taniguchi, K.-i. Katsumata, N. Matsushita, T. Kogure and K. Okada, *Cryst. Growth Des.*, 2011, **11**, 4831-4836.